Low-compressibility and hard materials ReB_2 and WB_2: Prediction from first-principles study

Xianfeng Hao,[1,3] Yuanhui Xu,[2] Zhijian Wu,[1] Defeng Zhou,[2] Xiaojuan Liu,[1] Xueqiang Cao,[1] and Jian Meng[1,*]
[1]*Key Laboratory of Rare Earth Chemistry and Physics, Changchun Institute of Applied Chemistry, Chinese Academy of Sciences, Changchun 130022, People's Republic of China*
[2]*School of Biological Engineering, Changchun University of Technology, Changchun 130012, People's Republic of China*
[3]*Graduate School, Chinese Academy of Sciences, Beijing 100049, People's Republic of China*
(Received 15 August 2006; revised manuscript received 22 October 2006; published 29 December 2006)

First-principle calculations are performed to investigate the structural, elastic, and electronic properties of ReB_2 and WB_2. The calculated equilibrium structural parameters of ReB_2 are consistent with the available experimental data. The calculations indicate that WB_2 in the $P6_3/mmc$ space group is more energetically stable under the ambient condition than in the $P6/mmm$. Based on the calculated bulk modulus, shear modulus of polycrystalline aggregate, ReB_2 and WB_2 can be regarded as potential candidates of ultra-incompressible and hard materials. Furthermore, the elastic anisotropy is discussed by investigating the elastic stiffness constants. Density of states and electron density analysis unravel the covalent bonding between the transition metal atoms and the boron atoms as the driving force of the high bulk modulus and high shear modulus as well as small Poisson's ratio.

DOI: 10.1103/PhysRevB.74.224112 PACS number(s): 71.20.Be, 61.50.Lt, 62.20.Dc, 71.15.Mb

A great effort is currently focused on the synthesis and characterization of so-called intrinsic superhard materials exhibiting simultaneously very low compressibilities, wide thermodynamic ranges of chemical stability, and high scratch resistance as well as surface durability.[1–5] Covalent materials are much better candidates for high hardness than ionic compounds because electrostatic interactions are omnidirectional and yield low bond bending force constants, which results in low shear modulus, and metallic materials because their shear strength is low.[4,5] One of the strategies employed for the development of ultrahard materials is to introduce small, covalent bond-forming atoms such as boron, carbon, nitrogen, and/or oxygen into transition metals that possess high bulk modulus but low hardness.[3–6] Some potential hard materials such as OsB_2 (Refs. 6–9) and RuB_2 (Ref. 9) have been proposed and investigated intensively.

Based on the first-principles calculations, in our previous work on trends in elasticity and electronic properties of 5*d* transition-metal diborides in the hypothetical OsB_2-type structure, we predicted that ReB_2 and WB_2 might be more potential candidates for ultra-incompressible and hard materials, comparison with OsB_2.[10] OsB_2-type structure forms in an orthorhombic lattice (space group *Pmmn*, No. 59) with two formula units per unit cell, in which two transition metal atoms occupy the 2*a* Wychoff site (0, 0, *z*) and four *B* atoms hold the 4*f* position (*x*, 0, *z*).[11] Experimentally, the ReB_2 and WB_2 are found in the hexagonal phase within $P6_3/mmc$ and $P6/mmm$ space group with few freedom of atomic positions,[12–14] as shown in Fig. 1. It is noted that hardness is related to the elastic and plastic properties of a material. There are three conditions that must be met in order for a material to be hard: high bulk modulus, high shear modulus, and the creation and motion of the dislocations must be as small as possible, which indicated that a superhard material should have a three-dimensional isotropic structure with fixed atomic positions and covalent or partially covalent ionic bonds.[4] Therefore, the hexagonal phases of the ReB_2 and WB_2 are expected to be harder than the hypothetical structure. However, much less is known about the mechanical properties of ReB_2 and WB_2. The reason for this can be attributed to difficulties in synthesizing bulk and/or single crystalline. First-principles calculation is one strong and useful tool to provide further details about the crystal structure and its properties related to the electron configuration of a material and therefore is highly desirable. So far no first-principles calculations for these two compounds were reported.

In this paper, we preformed density functional calculations to investigate the electronic and elastic properties of WB_2 and ReB_2 within the CASTEP code.[15] The exchange and correlation functional was treated by both the local density approximation (LDA-CAPZ) (Ref. 16) and the generalized gradient approximation (GGA-PBE).[17] The Vanderbilt ultrasoft pseudopotential[18] was used with the same cutoff energy of 400 eV; the *k* points of $10\times10\times4$ for ReB_2, $9\times9\times2$ for WB_2 in the $P6_3/mmc$ phase, and $9\times9\times8$ for WB_2 in the $P6/mmm$ phase are generated using the Monkhorst-Pack scheme.[19]

The calculated lattice constants for WB_2 and ReB_2, within

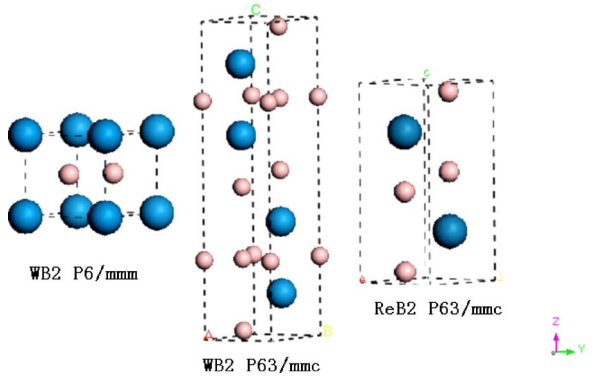

FIG. 1. (Color online) Crystal structures of WB_2 within the $P6/mmm$ and $P6_3/mmc$ space groups and ReB_2 in $P6_3/mmc$ space group. The transition metals W and Re atoms are presented as big spheres and the B atoms as small spheres, respectively.

TABLE I. Calculated equilibrium lattice parameters, a (Å), c (Å), equilibrium volume (Å^3), zero-pressure elastic constants C_{ij} (GPa), and density ρ (g/cm^3), heat of formation (eV), Debye temperature (K) compared with available experimental data for hexagonal WB_2 and ReB_2.

	$P6/mmm$ WB_2			$P6_3/mmc$ WB_2			$P6_3/mmc$ ReB_2		
	LDA	GGA	Expt.[a]	LDA	GGA	Expt.[b]	LDA	GGA	Expt.[c]
V[Å^3]	26.6899	26.7473	24.0904	110.7450	110.9476	106.961	52.7425	53.2613	54.4643
a[Å]	3.0532	3.0501	3.020	3.0404	3.0429	2.9831	2.8698	2.8809	2.900
c[Å]	3.3060	3.3197	3.050	13.8219	13.8357	13.8790	7.3946	7.4096	7.478
C_{11}	590.1	586.4		572.5	570.7		685.0	667.9	
C_{33}	442.8	419.3		658.9	672.1		1088.3	1062.7	
C_{44}	98.8	94.4		205.9	202.3		282.3	273.2	
$C_{66}=(C_{11}-C_{12})/2$	201.3	203.4		212.5	212.9		267.3	265.6	
C_{12}	187.4	183.7		147.4	144.7		150.5	136.7	
C_{13}	236.4	234.9		212.7	199.9		158.4	147.4	
ρ [g/cm^3]	12.7835	12.7561	14.1629	12.3235	12.3010	12.7595	13.0864	12.9589	12.6727
ΔH [eV]	0.1259	0.2588		−0.8798	−0.7592		−1.4205	−1.3240	
T_D [K]	624.2	615.4		748.2	749.7		866.4	858.3	

[a]Reference 14.
[b]Reference 13.
[c]Reference 12.

both LDA and GGA, are listed in Table I together with their corresponding experimental results. It is clear that the predicted lattice parameters are larger within GGA method than that within LDA method, as the usual case. The computed lattice parameters for hexagonal ReB_2 within GGA method are in a good accordant with the available experimental data:[12] the deviation between the experimental and theoretical values is less than 1%. In addition, the calculated density is overestimated by 2.2% compared with the experimental value of 12.6727 g/cm^3.[12] For WB_2 in the $P6_3/mmc$ space group, the computed lattice constants a and c deviate from the corresponding experimental values[13] within 2%, and the density within 3.5% when using GGA. While the theoretical lattice parameters a/c in the $P6/mmm$ space group are 3.0532/3.3060 and 3.0501/3.3197, within LDA and GGA, respectively. The highest disagreement in the lattice constant c (8% – 9%) is obtained for hexagonal WB_2 in the $P6/mmm$ phase, compared with the experimental data.[14] Here we shall emphasize that transition metal borides with metal-deficient or boron-deficient compositions can be easily obtained in the experiments. Furthermore, we found that the lowest energy, i.e., the ground state of the crystal, corresponds to the $P6_3/mmc$ phase for WB_2 from the relative heat of formation values.[20] The positive heat of formation for the $P6/mmm$ phase WB_2 indicated that it is energetically unstable, in contrast to the experimental observation.[14] The reason for this might be attributed to nonstoichiometric phase in experiments. Generally, the LDA underestimates the lattice constants while the GGA overestimates them when compared with experiments.[21] Here, even the GGA seems to underestimate the lattice constants. The slight underestimation of the calculated values can be related to the neglect of temperature effect and the nonstoichiometric effect in the present calculations. In one word, the agreement of the structural to published results confirms the accuracy and reliability of the computational procedure employed.

The accurate calculation of elasticity is essential for understanding the macroscopic mechanical properties of solids and for the design of hard materials. Therefore, the elastic coefficients were determined from first-principles calculation by applying a set of given homogeneous deformations with a finite value and calculating the resulting stress with respect to optimizing the internal atomic freedoms implemented by Milman *et al.*[22] Two strain patterns, one with nonzero ε_{11} and ε_{23} components, and the other with a nonzero ε_{23}, brought out stresses related to the all five independent elastic coefficients for the hexagonal unit cell. Three positive and three negative amplitudes are applied for each strain component with a maximum strain value of 0.3%. The calculated results are also shown in Table I. For a stable hexagonal structure, its five independent elastic constants C_{ij} (C_{11}, C_{12}, C_{13}, C_{33}, and C_{44} in Voigt notation) should satisfy the well-known Born stability criteria,[23] i.e., $C_{12}>0$, $C_{33}>0$, $C_{66}=(C_{11}-C_{12})>0$, $C_{44}>0$, and $(C_{11}+C_{12})C_{33}-2C_{13}^2>0$. Clearly, these calculated elastic constants C_{ij} satisfy the Born stability criteria, suggesting that the hexagonal phases of ReB_2 and WB_2 are mechanically stable.

As mentioned above, large single crystals of ReB_2 and WB_2 are currently unavailable and measurement of the individual elastic constants is not possible. However, on the basis of the Voigt-Reuss-Hill approximation,[24] we have calculated the corresponding bulk and shear moduli from the single crystal zero-pressure elastic constants, which may be determined on the polycrystalline samples experimentally. For specific cases of hexagonal lattices, the Reuss shear modulus (G_R) and the Voigt shear modulus (G_V) are given by

$$G_R = \frac{15}{4(2S_{11}+S_{33})-4(S_{12}+2S_{13})+3(2S_{44}+S_{66})}$$

and

TABLE II. Calculated isotropic bulk modulus B (GPa), shear modulus G (GPa), Young's modulus E (GPa), and Possion's ratio v and shear anisotropy ratio A, the ratio between linear compressibility coefficients k_c/k_a, and anisotropic factors A_G, A_B for hexagonal WB_2 and ReB_2.

	$P6/mmm$ WB_2		$P6_3/mmc$ WB_2		$P6_3/mmc$ ReB_2	
	LDA	GGA	LDA	GGA	LDA	GGA
G_R	129.5	124.3	206.2	207.4	290.7	285.2
G_V	144.0	140.6	207.0	208.1	299.1	293.5
$G_H=(G_R+G_V)/2$	136.7	132.5	206.6	207.7	294.9	289.4
B_R	324.1	317.7	323.4	318.2	361.3	346.7
B_V	327.0	322.1	327.7	322.5	377.2	362.4
$B_H=(B_R+B_V)/2$	325.6	319.9	325.6	320.4	369.2	354.5
E_H	359.7	349.3	511.6	512.4	698.7	682.5
v	0.3158	0.3180	0.2381	0.2335	0.1846	0.1791
$A=C_{44}/C_{66}$	0.49	0.46	0.97	0.95	1.06	1.03
k_c/k_a	1.48	1.63	0.66	0.67	0.56	0.56
A_G [%]	5.3	6.1	0.2	0.2	1.4	1.4
A_B [%]	0.4	0.6	0.6	0.6	2.1	2.2

$$G_V = \frac{1}{15}(2C_{11} + C_{33} - C_{12} - 2C_{13}) + \frac{1}{5}(2C_{44} + C_{66})$$

and the Ruess bulk modulus (B_R) and the Voigt bulk modulus (B_V) are defined as

$$B_R = \frac{1}{(2S_{11} + S_{33}) + 2(S_{12} + 2S_{13})}$$

and

$$B_V = \frac{1}{9}(2C_{11} + C_{33}) + \frac{2}{9}(C_{12} + 2C_{13}),$$

where the S_{ij} is the elastic compliance constants. Additionally, the Young modulus and Poisson's ratio are included, as presented in Table II.

It is acknowledged that bulk modulus or shear modulus can measure the hardness in an indirect way,[25] that is, materials with high bulk or shear modulus are likely to be hard materials. Our results demonstrate that within both LDA and GGA the values of the bulk modulus for ReB_2 and WB_2 are higher than the corresponding values for the hypothetical $Pmmn$ structure,[10] indicating the potential low compressible materials. Simultaneously, the induced shear moduli approach or exceed their counterpart values for the hypothetical phases.[10] Of the most interest, the shear modulus C_{44} of ReB_2 and WB_2 in the hexagonal phase within GGA, which relates to lattice resistance against an applied $[11\bar{2}0]$ (0001) shear deformation, are 273 and 202 GPa, while the corresponding values are 214 and 184 GPa.[10] Jhi *et al.*[26] proved that the magnitude of the shear modulus C_{44}, rather than the bulk modulus B and shear modulus G, was a better hardness predictor for transition-metal carbonitrides. If this is true for the present studied compounds, the high values of C_{44} for ReB_2 and WB_2 might also support our expectations. An important conclusion we can draw from the graph is that ReB_2 and WB_2 in the $P6_3/mmc$ phase might be potential candidates for ultra-incompressible and hard materials. Owning to their potential significance in this respect, experimental studies on structural and mechanical properties are strongly recommended.

It is well known that microcracks are easily induced in the materials due to the significant elastic anisotropy.[27] Hence, it is important to calculate elastic anisotropy in order to improve their mechanical durability. We calculated the shear anisotropy ratio A, $A=C_{44}/C_{66}$,[28] for the two compounds. ReB_2 is stiffer against shear modes ε_{13} or ε_{23} than ε_{12} with respect to A within the range of 1.02–1.06, being slightly larger than 1, whereas WB_2 possesses an opposite shear anisotropy property for A between 0.95 and 0.97, smaller than 1. The knowledge of elastic coefficients also provides a method to evaluate the linear compressibility. The ratio between linear compressibility coefficients k_c/k_a of hexagonal crystal can be expressed as[29]

$$k_c/k_a = (C_{11} + C_{12} - 2C_{13})/(C_{33} - C_{13}).$$

The implication of the definition is that a value of unity corresponds to the isotropic compressibility, while the deviation from the unity is a measure of the degree of anisotropy for the linear compressibility along the c and a direction. The k_c/k_a of ReB_2 and WB_2 is about 0.56 and 0.66, respectively. These values suggested that the compressibility along the c axis is much smaller than the a axis in both compounds which agrees well with the calculated elastic constants along different axis (shown in Table I) and the ReB_2 is more anisotropic than WB_2. The anisotropic elasticity can be understood in terms of the hexagonal structure. In the ab plane, the boron and the transition metal atoms are in planes that are offset from each other; therefore, the electrostatic repulsion did not push each other directly, and then could not maximize incompressibility. In contrast, along the c axis, the boron and the transition metal atoms are directly aligned, leading to highly directional repulsive electronic interactions, and then the least compressible. Alternatively, Chung and

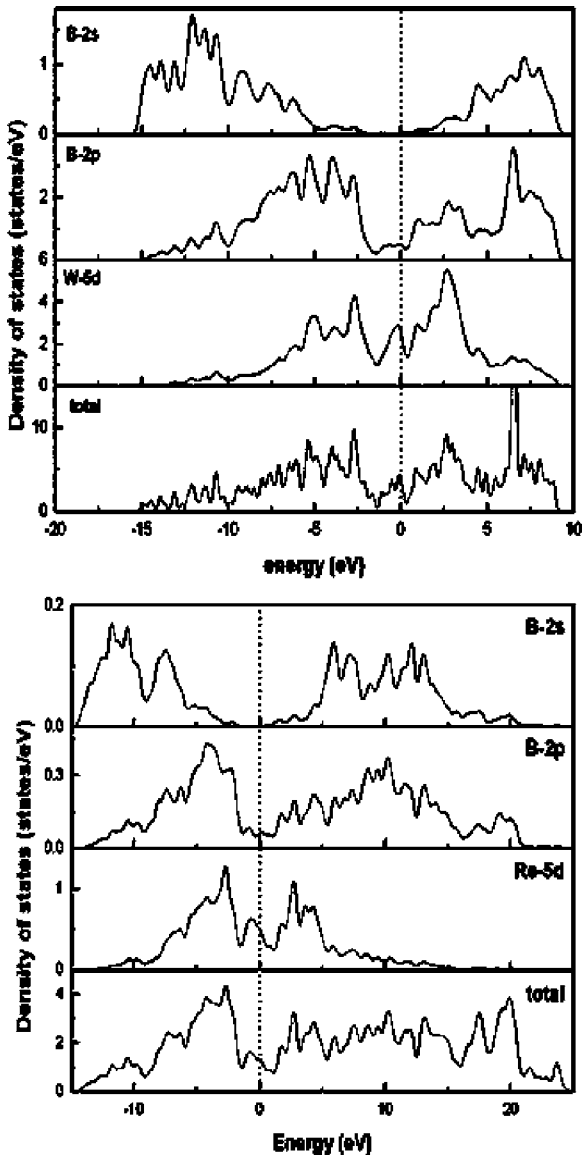

FIG. 2. Total and partial density of states of WB_2 and ReB_2 in the $P6_3/mmc$ space group. The dotted line at zero is the Fermi energy level.

Buessem[30] introduced percent elastic anisotropy for polycrystalline materials which is defined as

$$A_B = (B_V - B_R)/(B_V + B_R) \quad \text{and} \quad A_G = (G_V - G_R)/(G_V + G_R)$$

in compressibility and shear, respectively. Where B and G denote the bulk and shear modulus, and the subscripts V and R represent the Voigt and Reuss approximation. For these expressions, a value of zero identifies elastic isotropy and a value of 100% corresponds to the largest possible anisotropy. Compared the average A_B=2.2% with A_G=1.4% for ReB_2, we find much anisotropy in compressibility than in shear. For WB_2, A_B=0.6% and A_G=0.2%, indicate almost elastic isotropy, and these small values demonstrate WB_2 is less anisotropic than ReB_2, as stated above. However, WB_2 in the $P6/mmm$ phase, hold opposite shear anisotropy and linear compressibility coefficients is correlated to the different

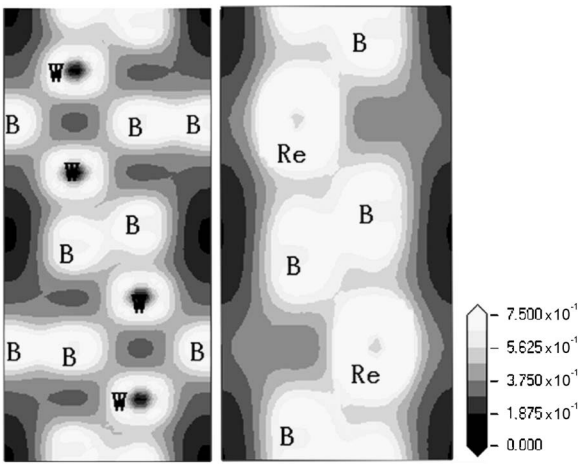

FIG. 3. The valence electron density for WB_2 (left) and ReB_2 (right) in $(11\bar{2}0)$ plane in $P6_3/mmc$ space group. The bonding between W/Re and B exhibits the strong directionality throughout the plane.

atomic arrangement in the structure, compared with the $P6_3/mmc$ phase.

The Debye temperature is a fundamental parameter of a material which is link to many physical properties such as specific heat, elastic constants, and melting point.[27] It can be obtained from the average sound velocity using the following equation:

$$T_D = \frac{h}{k}\left[\frac{3n}{4\pi}\left(\frac{N_A\rho}{M}\right)\right]^{1/3} v_m.$$

Here h is Plank's constant, k is Boltzmann's constant, N_A is Avogadro's number, ρ is density, M is the molecular weight and n is the number of atoms in the molecule. The average wave velocity v_m is approximately estimated by the equation

$$v_m = \left[\frac{1}{3}\left(\frac{2}{v_t^3} + \frac{1}{v_l^3}\right)\right]^{-1/3},$$

where v_l and v_t are longitudinal and transverse elastic wave velocity of the polycrystalline materials and can be obtained using the polycrystalline shear modulus and bulk modulus from Navier's equation.[31] The calculated values of Debye temperatures are listed in Table I. Our results predict that T_D is higher for ReB_2 than for WB_2, suggesting that ReB_2 is harder than WB_2. LDA values are slightly larger than those obtained within GGA due to the tendency to overestimate the bonding. In addition, the calculated values are higher than the corresponding values for the hypothetical phases,[10] supporting our expectations.

To understand the mechanical properties of these two materials on a fundamental level, the density of states (DOS) and electron density are calculated at zero pressure within the LDA and GGA method. We find that the density of states and electron density calculated using both the LDA and the GGA methods at the corresponding equilibrium lattice constants show similar patterns. Hence, in this paper, as a matter of convenience only, the GGA results are presented in all figures.

The site projected and total density of states (DOS) for WB_2 and ReB_2 are shown in Fig. 2 where the vertical line indicates Fermi level E_F. The DOS of TM-5*d* and B-2*p* are energetically degenerate from the bottom of valence band to the Fermi level, indicating the covalent hybridization between TM and B atom in these compounds. It is found that the electrons from TM-5*d* and B-2*p* states both contribute to the density of states at the Fermi level; hence these two compounds exhibit metallic behavior. The typical feature of the total DOS of these compounds is the presence of what is called as a pseudogap which is considered as the borderline between the bonding states and antibonding states.[7–10] It should be pointed out that the E_F is lying on the pseudogap in ReB_2 and WB_2, indicating the *p*-*d* bonding states started to be saturated. The nearly full occupation of the bonding states and without filling on the antibonding states results in the high bulk modulus and shear modulus, small Poisson's ratio.[10] To gain a more detailed insight into the bonding characters of these compounds, we plot the charge density distribution in $(11\bar{2}0)$ plane, as shown in Fig. 3. From that we can see some electrons between the transition metal atoms and the boron atoms, indicating a strong directional covalent TM–B bonding exists in these ReB_2 and WB_2 compounds. Furthermore, two neighbor boron atoms form a very strong covalent bond. It is emphasized that the formation of these directional covalent bonds leads to the increase in the hardness.

In conclusion, by performing first-principles plane-wave pseudopotential total energy calculations, we studied the structural, elastic, and electronic properties of ReB_2 and WB_2. Our calculated equilibrium structural parameters of ReB_2 are consistent with the experimental results. The relative values of heat of formation indicated that WB_2 in $P6_3/mmc$ space group is more energetically stable than in the $P6/mmm$ space group under the ambient condition. The computed bulk modulus and shear modulus suggested that they are potential low compressible and hard materials. In addition, these two compounds show different degrees of elastic anisotropy. Density of states and electron density analysis unravel the covalent bonding between the transition metal atoms and the boron atoms as the driving force of the high bulk modulus and high shear modulus as well as small Poisson's ratio. We hope that these calculations will stimulate experimental work on these technologically very interesting materials.

The authors thank the National Natural Science Foundation of China for financial support (Grant Nos. 20331030, 20571073, 20671088, and 20661026). The authors wish to express thanks to Yanshan University for the computer time.

*Corresponding author. Electronic address: jmeng@ciac.jl.cn

[1] V. L. Solozhenko, D. Andrault, G. Fiquet, M. Mezouar, and D. C. Rubie, Appl. Phys. Lett. **78**, 1385 (2001).
[2] A. G. Thornton and J. Wilks, Nature (London) **274**, 792 (1978).
[3] J. J. Gilman, R. W. Cumberland, and R. B. Kaner, Int. J. Refract. Met. Hard Mater. **24**, 1 (2006).
[4] J. Haines, J. M. Léger, and G. Bocquillon, Annu. Rev. Mater. Res. **31**, 1 (2001).
[5] R. B. Kaner, J. J. Gilman, and S. H. Tolbert, Science **308**, 1268 (2005).
[6] R. W. Cumberland, M. B. Weinberger, J. J. Gilman, S. M. Clark, S. H. Tolbert, and R. B. Kaner, J. Am. Chem. Soc. **127**, 7264 (2005).
[7] H. Y. Gou, L. Hou, J. W. Zhang, H. Li, G. F. Sun, and F. M. Gao, Appl. Phys. Lett. **88**, 221904 (2006).
[8] Z. Y. Chen, H. J. Xiang, J. Yang, J. G. Hou, and Q. S. Zhu, Phys. Rev. B **74**, 012102 (2006).
[9] S. Chiodo, H. J. Gotsis, N. Russo, and E. Sicilia, Chem. Phys. Lett. **425**, 311 (2006).
[10] X. F. Hao, Z. J. Wu, X. J. Liu, and J. Meng, Phys. Rev. B (to be published).
[11] B. Aronsson, Acta Chem. Scand. (1947-1973) **17**, 2036 (1963).
[12] S. La Placa and B. Post, Acta Crystallogr. **15**, 97 (1962).
[13] T. Lundström, Ark. Kemi **30**, 115 (1969).
[14] H. P. Woods, F. E. Wawner, Jr., and B. G. Fox, Science **151**, 75 (1966).
[15] MATERIALS STUDIO, Version 2.1.5, Accelrys Inc., 2002.
[16] D. M. Ceperley and B. J. Alder, Phys. Rev. Lett. **45**, 566 (1980); J. P. Perdew and Y. Wang, Phys. Rev. B **45**, 13244 (1992).
[17] J. P. Perdew, K. Burke, and M. Ernzerhof, Phys. Rev. Lett. **77**, 3865 (1996).
[18] M. D. Segall, P. J. D. Lindan, M. J. Probert, C. J. Pickard, P. J. Hasnip, S. J. Clark, and M. C. Payne, J. Phys.: Condens. Matter **14**, 2717 (2002).
[19] J. D. Pack and H. J. Monkhorst, Phys. Rev. B **16**, 1748 (1977).
[20] The heat of formation, calculated by subtracting the calculated energy of the pure elemental constituents (E^{TM}_{solid} and E^{B}_{solid}) from the crystal total energy ($E^{TMB_2}_{total}$).
[21] P. Lukashev and W. R. L. Lambrecht, Phys. Rev. B **70**, 245205 (2004).
[22] V. Milman and M. C. Warren, J. Phys.: Condens. Matter **13**, 241 (2001).
[23] M. Born, Proc. Cambridge Philos. Soc. **36**, 160 (1940).
[24] R. Hill, Proc. Phys. Soc. London **65**, 349 (1952).
[25] D. M. Teter, MRS Bull. **23**, 22 (1998).
[26] S-H. Jhi, J. Ihm, S. G. Louie, and M. L. Cohen, Nature (London) **399**, 132 (1999); Z. G. Wu, X. J. Chen, V. V. Struzhkin, and R. E. Cohen, Phys. Rev. B **71**, 214103 (2005).
[27] P. Ravindran, L. Fast, P. A. Korzhavyi, B. Johnnsson, J. Wills, and O. Eriksson, J. Appl. Phys. **84**, 4891 (1998).
[28] J. Y. Wang and Y. C. Zhou, Phys. Rev. B **69**, 144108 (2004).
[29] J. Y. Wang, Y. C. Zhou, T. Liao, and Z. J. Lin, Appl. Phys. Lett. **89**, 021917 (2006).
[30] D. H. Chung and W. R. Buessem, in *Anisotropy in Single Crystal Refractory Compound*, edited by F. W. Vahldiek and S. A. Mersol (Plenum, New York, 1968), Vol. 2, p. 217.
[31] E. Schreiber, O. L. Anderson, and N. Soga, *Elastic Constants and their Measurements* (McGraw-Hill, New York, 1973).